


## ORIGINAL ARTICLE

# Mechanism of interaction between hydroxypropyl cellulose and water in aqueous solutions: Importance of polymer chain length

Manuel Martin-Pastor<sup>1</sup> | Edmont Stoyanov<sup>2</sup> 

<sup>1</sup>Unidad de Resonancia Magnética,  
University of Santiago de Compostela,  
RIAIDT, Santiago de Compostela, Spain

<sup>2</sup>Nisso Chemical Europe, Duesseldorf,  
Germany

**Correspondence**

Edmont Stoyanov, Nisso Chemical  
Europe, Berliner Allee 42, 40212  
Duesseldorf, Germany.  
Email: stoyanov@nisso-chem.de

**Abstract**

The utilization of hydroxypropyl cellulose (HPC) can be regarded as unexpected with regard to certain applications, such as being employed as a solubility enhancer for poorly soluble drugs and as a solubilizing agent for nano-suspensions and amorphous solid dispersions. However, the best results were obtained for low-molecular weight ( $M_w$ ) HPC grades with a short-chain structure. Therefore, in this study, seven grades of HPC with different polymer chain lengths ( $M_w$ ) are analyzed in various aqueous solutions by a combination of <sup>1</sup>H quantitative NMR spectroscopy, diffusion NMR spectroscopy, and water ligand observed via gradient spectroscopy; these investigations provide insights into the remarkable solubilizing property of HPC at the molecular and supramolecular levels. Furthermore, the hydration and the water residence time are found to be strongly dependent on the polymer chain length of HPC. The quantitative results obtained herein indicate that HPCs with shorter chain lengths retain smaller amounts of water around their hydrated molecules, as compared to their counterparts with longer chain lengths.

**KEYWORDS**

<sup>1</sup>H water ligand observed via gradient spectroscopy (WaterLOGSY), diffusion-oriented spectroscopy (DOSY), hydroxypropyl cellulose, quantitative perfect-echo Watergate <sup>1</sup>H-NMR, variable temperature NMR

## 1 | INTRODUCTION

Hydroxypropyl cellulose (HPC) is a cellulose ether often used in pharmaceuticals as a tablet binder and film-coating agent. Recent studies have demonstrated new and unexpected features of these polymers as solubility enhancers for poorly soluble drugs as well as for solubilizing nano-suspensions and amorphous solid dispersions.<sup>[1–3]</sup> These studies revealed that the best results could be achieved

with low-molecular weight ( $M_w$ ) polymers corresponding to short-chain HPC grades.

The chemical structure of HPC has been investigated in the past by <sup>1</sup>H and <sup>13</sup>C NMR spectroscopies.<sup>[4,5]</sup> Kimura et al.<sup>[4]</sup> elucidated the degree of substitution, molecular substitution, and the different reactivities of the hydroxyl groups in cellulose molecules based on the <sup>13</sup>C-NMR peak integrals of samples prepared in D<sub>2</sub>O. Using the same carbon NMR method, Desai et al.<sup>[5]</sup> analyzed the performance

This is an open access article under the terms of the Creative Commons Attribution License, which permits use, distribution and reproduction in any medium, provided the original work is properly cited.

© 2020 The Authors. *Journal of Polymer Science* published by Wiley Periodicals LLC.

of HPCs comprising different cloud points, with an emphasis on the ratio of outer/single carbons versus inner carbons. These fundamental works assumed that the HPC molecular structure is independent of the polymer chain length and that the examined grades in these studies are representative of the entire HPC family.

However, the reasons for the better solubilizing characteristics of low  $M_w$  HPC grades for poorly soluble drugs have not been clearly understood yet. There are no meaningful differences in the physicochemical properties (solubility, dynamic light scattering, mass spectrometry, and inner/outer carbon ratio) of different grades of this cellulose ether. To obtain meaningful insights on the HPC behavior in aqueous solutions and the effect of molecular weight at the molecular and supramolecular levels, we employed NMR techniques to quantitatively study the self-aggregation properties of HPC in solution and the accessibility of water in different parts of the polymer structure. To comprehensively study these effects, we analyze and compare the results obtained for seven different HPC grades with different molecular weights (chain lengths).

## 2 | EXPERIMENTAL METHODS

### 2.1 | Chemicals

Seven HPC grades with average molecular weights of 2,500,000 (HPC-VH), 1,000,000 (HPC-H), 700,000 (HPC-M), 140,000 (HPC-L), 100,000 (HPC-SL), 40,000 (HPC-SSL), and 20,000 (HPC-UL) were procured from Nippon Soda (Japan), for this study.

### 2.2 | Experiments

NMR experiments were conducted on a Bruker NEO 17.6 T spectrometer (proton resonance at 750 MHz) equipped with a  $^1\text{H}/^{13}\text{C}/^{15}\text{N}$  triple resonance probe and a shielded PFG z-gradient. TopSpin 4.0 was used as the control software. All the spectra were processed using MestreNova v12.0 (Mestrelab Research, Inc.). Chemical shifts were referenced automatically against a deuterium lock. All spectra were recorded at 25°C unless otherwise indicated.

#### 2.2.1 | Sample preparation

Samples of HPC-VH, HPC-H, HPC-M, HPC-L, HPC-SL, HPC-SSL, and HPC-UL were prepared at mol/mol concentration of 1.8% in  $\text{D}_2\text{O}$  (D 99.9%) (Eurisotop, Inc.). Subsequently, 500  $\mu\text{l}$  of the samples were transferred to the 5 mm standard NMR tubes. For recording the water

ligand observed via gradient spectroscopy (WaterLOGSY) spectra,<sup>[6]</sup> similar sample concentrations and volumes were used. Unless otherwise indicated, the NMR spectra discussed in this study refer to the samples prepared in  $\text{D}_2\text{O}$ .

Samples of HPC-VH, HPC-H, HPC-M, HPC-L, HPC-SL, HPC-SSL, and HPC-UL were prepared at mol/mol concentration of 1.8% in  $\text{D}_2\text{O}$  (D 99.9%) (Eurisotop, Inc.). Subsequently, 500  $\mu\text{l}$  of the samples were transferred to the 5 mm standard NMR tubes. For recording the water ligand observed via gradient spectroscopy (WaterLOGSY) spectra,<sup>[6]</sup> similar sample concentrations and volumes were used. Unless otherwise indicated, the NMR spectra discussed in this study refer to the samples prepared in  $\text{D}_2\text{O}$ .

#### 2.2.2 | Variable temperature quantitative $^1\text{H}$ spectra

Proton quantitative monodimensional spectra ( $^1\text{H}$ ) of the seven prepared HPC samples were recorded at 25 and 40°C. Each spectrum was recorded over 128 scans with a pulse-acquisition sequence using an interscan delay ( $d_1$ ) of 10 s and acquisition time (aq) of 2.75 s. Each spectrum was processed and analyzed by integration of the area corresponding to aliphatic protons ( $\delta$  from 0.5 to 1.3 ppm), pyranose ring protons ( $\delta$  from 2.88 to 4.17 ppm), and a residual water peak (HDO) at  $\sim 4.7$  ppm in the spectrum measured at 25°C and 4.5 ppm at 40°C. In each spectrum, peak areas were normalized with respect to the integral of the HDO peak; the signal (100%) enhancement factor was calculated independently for the peaks of pyranose rings and aliphatic chains using Equation (1),

$$\text{Enh}_A = (\text{Int}_A^{40\text{C}} / \text{Int}_{\text{HDO}}^{40\text{C}}) / (\text{Int}_A^{25\text{C}} / \text{Int}_{\text{HDO}}^{25\text{C}}), \quad (1)$$

where  $\text{Int}_A^{40\text{C}}$  and  $\text{Int}_A^{25\text{C}}$  refer to the integrals of peak A in the NMR spectra measured at 40°C and 25°C, respectively. In this case, the two peaks of interest corresponded with the pyranose ring protons and aliphatic protons.  $\text{Int}_{\text{HDO}}^{40\text{C}}$  and  $\text{Int}_{\text{HDO}}^{25\text{C}}$  refer to the normalized integrals of HDO in the NMR spectra recorded at 40°C and 25°C, respectively.

#### 2.2.3 | Diffusion NMR spectrum

DOSY (pulse sequence *ledbpgp2s* of the Bruker library)<sup>[7]</sup> analysis of the seven chosen HPC samples was conducted with the BiPolar-Gradients-Longitudinal Eddy Current

Compensated-Stimulated-Echo (BPP-LED-STE) experiments. Gradient pulses encoding diffusion were varied linearly from 1 to 50 G/cm along 32 points in the diffusion dimension. The duration of each pair of bipolar gradients  $\delta$  was 8 ms and the diffusion time  $\delta$  was 300 ms. Spectra were acquired with a relaxation delay ( $d_1$ ) of 3 s, acquisition time of 2.75 s, and 16 scans at each point in the diffusion dimension. After Fourier transformation in the  $^1\text{H}$  dimension, several peaks were selected for analyzing self-diffusion coefficients. In each case, peak intensity along the diffusion dimension was fitted to the mono-exponential Stejskal-Tanner equation by using the Origin v8.0 software to determine the self-diffusion coefficient ( $D$ ).

### 2.2.4 | Quantitative $^1\text{H}$ perfect-echo spectra

One-dimensional  $^1\text{H}$  quantitative perfect-echo Watergate spectra ( $^1\text{H}$  quantitative)<sup>[8]</sup> were recorded over 128 scans for the seven samples prepared in  $\text{H}_2\text{O}$  as the solvent. The interscan relaxation delay ( $d_1$ ) was 10 s while the acquisition time (aq) was 1.38 s.

### 2.2.5 | WaterLOGSY spectra

One-dimensional WaterLOGSY<sup>[6]</sup> spectra (pulse sequence *WaterLOGSY* of the Bruker library) were recorded for the seven chosen HPC samples dissolved in  $\text{H}_2\text{O}$ . A  $180^\circ$  inversion pulse was applied over the  $\text{H}_2\text{O}$  signal ( $\sim 4.7$  ppm) using a *sinc*-shaped selective pulse of 7.5 ms and bandwidth of 75 Hz. The strong water peak was suppressed before detection by using a pair of excitation-sculpting echoes based on a selective  $180^\circ$  Gaussian shaped refocusing pulse of 2 ms with PFG gradients of 1 ms duration and power levels of 31 and 11 G/cm. The spectra were recorded over 256 scans with interscan relaxation delay ( $d_1$ ) and acquisition times (aq) of 4 s and 1.38 s, respectively. Furthermore, WaterLOGSY spectra were acquired for each sample at the mixing times of 50, 100, 150, 300, and 500 ms.

## 3 | RESULTS AND DISCUSSION

### 3.1 | NMR study of the self-aggregation properties of HPC samples

Thermal gelation is a general property of aqueous HPC solutions (as shown in Figure 1) due to which, upon heating, aqueous solutions precipitate and form gels.

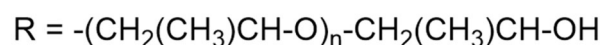
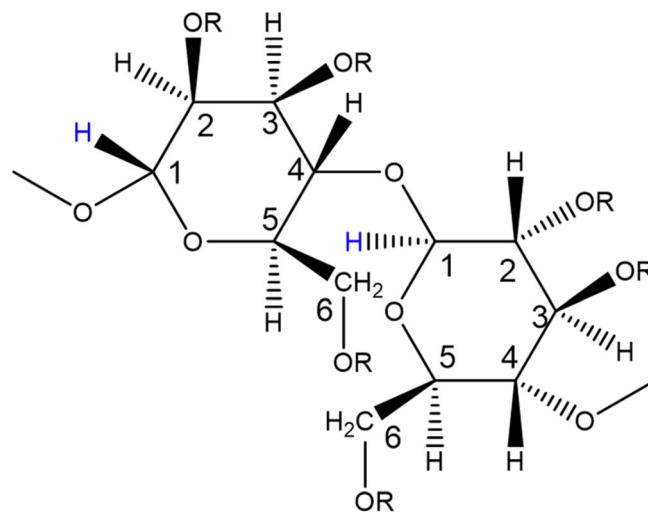


**FIGURE 1** Idealized chemical structure of HPC [Color figure can be viewed at [wileyonlinelibrary.com](http://wileyonlinelibrary.com)]

Gel formation is a completely reversible process and gelled samples liquefy once again upon cooling.<sup>[9,10]</sup> This characteristic depends primarily on molecular weight, degree of methyl and hydroxypropyl substitution, concentration, and the nature of additives. At the molecular level, gelation is a consequence of the formation of self-aggregates of HPC molecules in solution due to favorable hydrophobic interactions.<sup>[9,10]</sup>

The self-aggregation ability of the seven chosen HPC samples was studied at a constant concentration using two types of NMR. The first is concerned with recording the DOSY spectra to measure the  $D$  values of the most abundant species in solution. Depending on sample characteristics, the value of  $D$  obtained under a certain set of experimental conditions (concentration and temperature) reflects either the monomer species or an average of the several types of self-aggregates formed in solution. The average values of  $D$  obtained are shown in Table 1.

A representative DOSY spectrum of HPC-H is shown in Figure 2. The  $D$  values shown in Table 1 are sensitive to  $M_w$ . The viscosity of these polymers was measured by analytical techniques such as GPC. Furthermore, the inverse correlation between viscosity and  $M_w$  can also be inferred from the given values.

However, if the NMR values of  $D$  are converted into molecular weight ( $M_w^{\text{NMR}}$ ) using the empirical relationship proposed by Viel et al. for polysaccharides ( $D = 8.2 \times 10^{-9} M_w^{-0.49}$ ),<sup>[12]</sup> the results in Table 1 show a large discrepancy between  $M_w^{\text{NMR}}$  and  $M_w$ , as measured by GPC.  $M_w^{\text{NMR}}$  values are overestimated, which strongly suggests the possibility of self-aggregation under the experimental conditions used for recording NMR spectra in  $\text{D}_2\text{O}$ .

**TABLE 1** Comparison of the analytical and NMR data of the seven chosen HPC samples

	HPC-VH	HPC-H	HPC-M	HPC-L	HPC-SL	HPC-SSL	HPC-UL
$M_w$ (kDa) <sup>a</sup>	2,500	1,000	700	140	100	40	20
Avg. monomers	3,100	1,200	870	170	120	50	25
Viscosity (mPa·s)	4,001–6,000	1,000–4,000	150–400	6.0–10.0	3–5.9	2.0–2.9	1.0–1.9
NMR DOSY $D$ ( $\times 10^{-10}$ m <sup>2</sup> /s)	<0.01	0.02	0.05	0.12	0.18	0.34	0.48
$M_w^{\text{DOSY}}$ (kDa) <sup>b</sup>	>20,000	20,000	3,630	600	250	72	36
NMR VT- <sup>1</sup> H Enh_pyranose	1.81	3.76	3.76	1.06	1.09	1.46	1.11
NMR VT- <sup>1</sup> H Enh_aliphatic	1.38	1.34	1.38	1.34	1.20	1.06	0.93
NMR aliphatic to pyranose ratio <sup>c</sup>	1.29	1.13	1.24	0.99	0.85	0.81	0.79
NMR hydration %H <sub>2</sub> O hydr <sup>d</sup>	9%	1%	1%	81%	81%	92%	94%
NMR hydration %aliphatics <sup>e</sup>	36%	93%	94%	8%	7%	2%	0%

Abbreviations: HPC, hydroxypropyl cellulose; VT, variable temperature; WaterLOGSY, <sup>1</sup>H water ligand observed via gradient spectroscopy.

<sup>a</sup>Measured by GPC.

<sup>b</sup> $M_w^{\text{DOSY}}$  NMR is the molecular weight calculated from the diffusion coefficient  $D$ , which is measured from the DOSY spectrum by using the empirical relationship for polysaccharides, namely:  $D = 8.2 \times 10^{-9} M_w^{-0.49}$ .<sup>[11]</sup>

<sup>c</sup>Calculated by the integration of the <sup>1</sup>H quantitative spectra (Figure 3a), which is achieved by dividing the integral of the aliphatic signal by the integral of the pyranose ring signal in the same spectrum.

<sup>d</sup>Determined from the <sup>1</sup>H WaterLOGSY spectra by studying the points (h)–(n) in Figure 4 at 50 ms. Signal integral corresponding to H<sub>2</sub>O (hydr) is divided by the total area of signals in the same spectrum and is expressed in %.

<sup>e</sup>Determined from the <sup>1</sup>H WaterLOGSY spectra by studying the points (h)–(n) in Figure 4 at 50 ms. The integral of the aliphatic signal is divided by the total signal area in the same spectrum and is expressed as %.

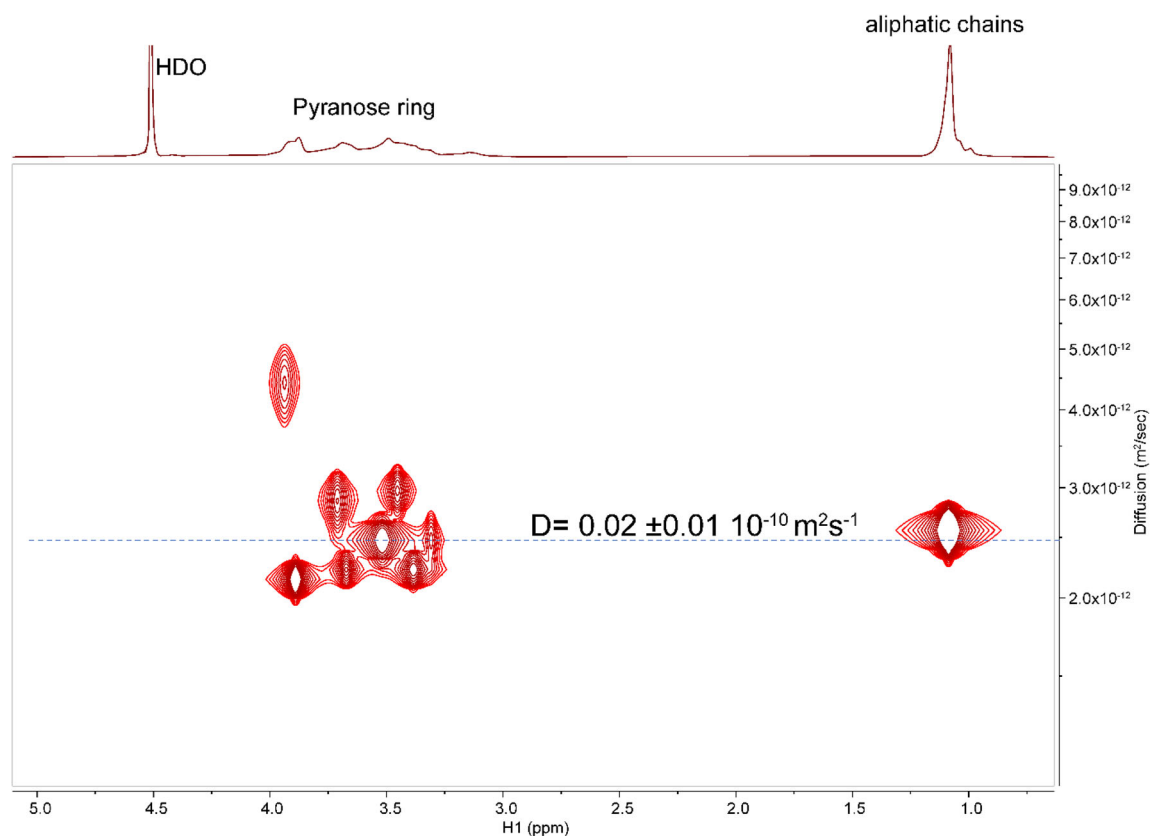


**FIGURE 2** Measurement of the diffusion coefficient of HPC-H prepared in D<sub>2</sub>O from its DOSY spectrum [Color figure can be viewed at [wileyonlinelibrary.com](http://wileyonlinelibrary.com)]

To clarify the issue of self-aggregation and the size of the species formed in the NMR samples, variable temperature (VT)  $^1\text{H}$  NMR quantitative spectra were recorded. We propose that in the solution state, the NMR signals of large species are broad due to their excessively slow rotational dynamics. Their broad signal leads to a reduction in the maximum peak intensity and as a result, a part of or the complete area of the peak may be below the noise level of the spectrum and is partially or completely “invisible.” This is an effect that has been previously reported for several polysaccharides.<sup>[13]</sup> Signals in the so-called invisible regime obviously do not contribute to the experimental integral measured in the spectrum and hence we only observe an apparent integral.

The VT technique is useful for studying dynamic processes in NMR and in this study, we employed it to detect the invisible signals of large species. In general, temperature modulates the rotational dynamics of molecules in a solution. Upon increasing the temperature, the rotational dynamics of large species are expected to increase and as a result, it is possible for a part of its integral to shift from the invisible regime to the visible regime causing a measurable increase in the (apparent) integral of the signals in the spectrum. The situation is similar in large self-aggregates, but the effect of

temperature on the apparent integral is more dramatic due to the increase in rotational dynamics; this may also affect their self-aggregation equilibrium, causing deaggregation to a certain extent. In the VT  $^1\text{H}$  NMR spectra of the seven HPC samples dissolved in  $\text{D}_2\text{O}$ , the integral area of the HDO peak was measured along with the area of the pyranose ring protons and aliphatic protons at 25 and 40°C. The HDO peak signal was used for normalization, as the area of this signal is not expected to change significantly in the relatively diluted samples (1.8%) used for testing. The case of HPC-H in Figure 3 exemplifies the results of VT  $^1\text{H}$  NMR studies obtained for the seven HPC samples considered.

Increasing the temperature from 25 to 40°C causes a notable increase in the peak integrals corresponding to the pyranose ring (factor 3.76 times in Table 1) and aliphatic chain (factor 1.35 times in Table 1) (Figure 3). Interestingly, these results show that at 40°C, the increase in the peak-integral area was 2.8 times more for the pyranose ring when compared to aliphatic chains; this observation can be attributed to differences in their flexibility (i.e., relatively faster rotational dynamics due to internal motion) when forming aggregates. The pyranose rings are taking part in the aggregation and are more rigid (or flexible) at the lower (or higher) temperatures. A similar phenomenon

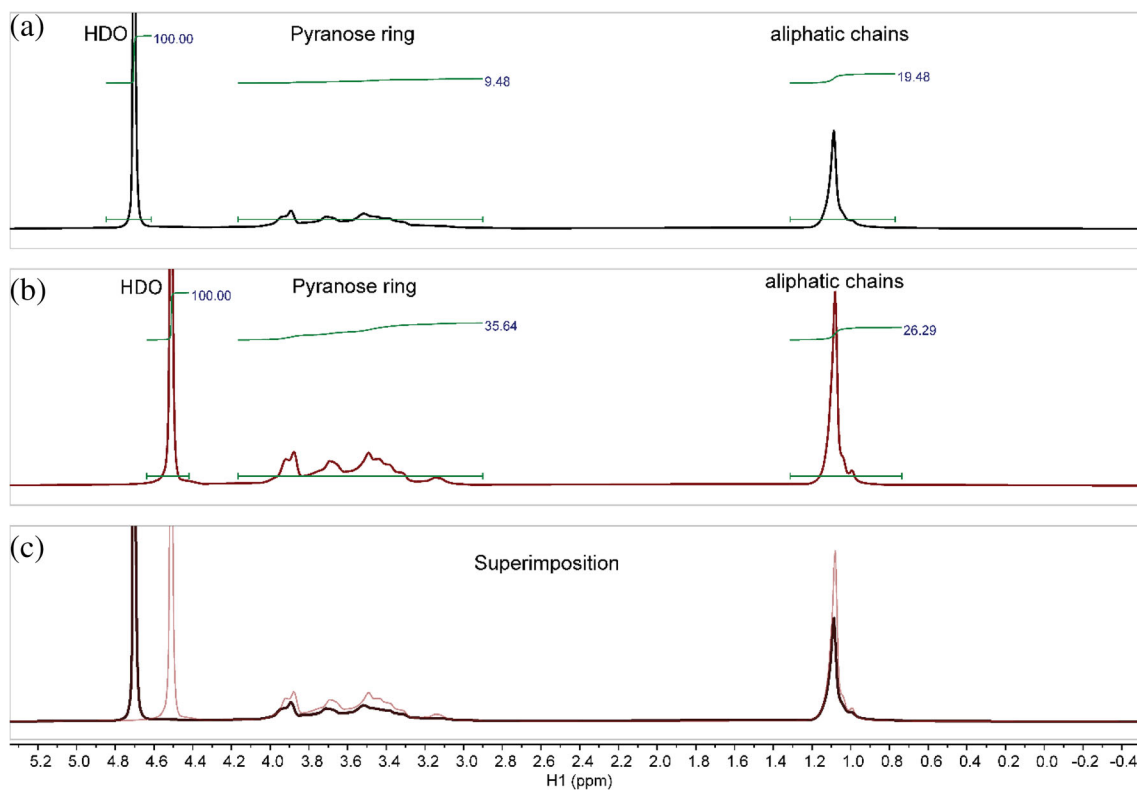


**FIGURE 3** VT  $^1\text{H}$  spectrum of HPC-H at (a) 25°C, (b) 40°C, and (c) superimposition of the spectra at 25 and 40°C with the same vertical scale for the HDO peak. In (a, b), the integrals of signals corresponding to HDO, pyranose rings, and aliphatic chains are shown; these signals are normalized with respect to the HDO peak [Color figure can be viewed at [wileyonlinelibrary.com](http://wileyonlinelibrary.com)]

was reported during NMR analysis of the pendant chains of acetyl groups in partially acetylated chitosan.<sup>[13]</sup> The enhancement factors obtained from the VT  $^1\text{H}$  quantitative spectra of the seven HPC samples are listed in Table 1. The trend observed in all these results was similar; they showed either no change in the degree of aggregation in the sample (signal enhancement factor of  $\sim 1$ ) or a significant reduction in aggregation at higher temperatures (signal enhancement factor  $> 1$ ). This unexpected result contrasts with the

reported effect of gellification occurring in other types of HPC samples at  $40^\circ\text{C}$  but not at  $25^\circ\text{C}$ .

### 3.2 | NMR analysis of hydration in HPC samples

The major characteristics of cellulose are water retention, adhesion, and lubrication. In this context, HPCs exhibit a

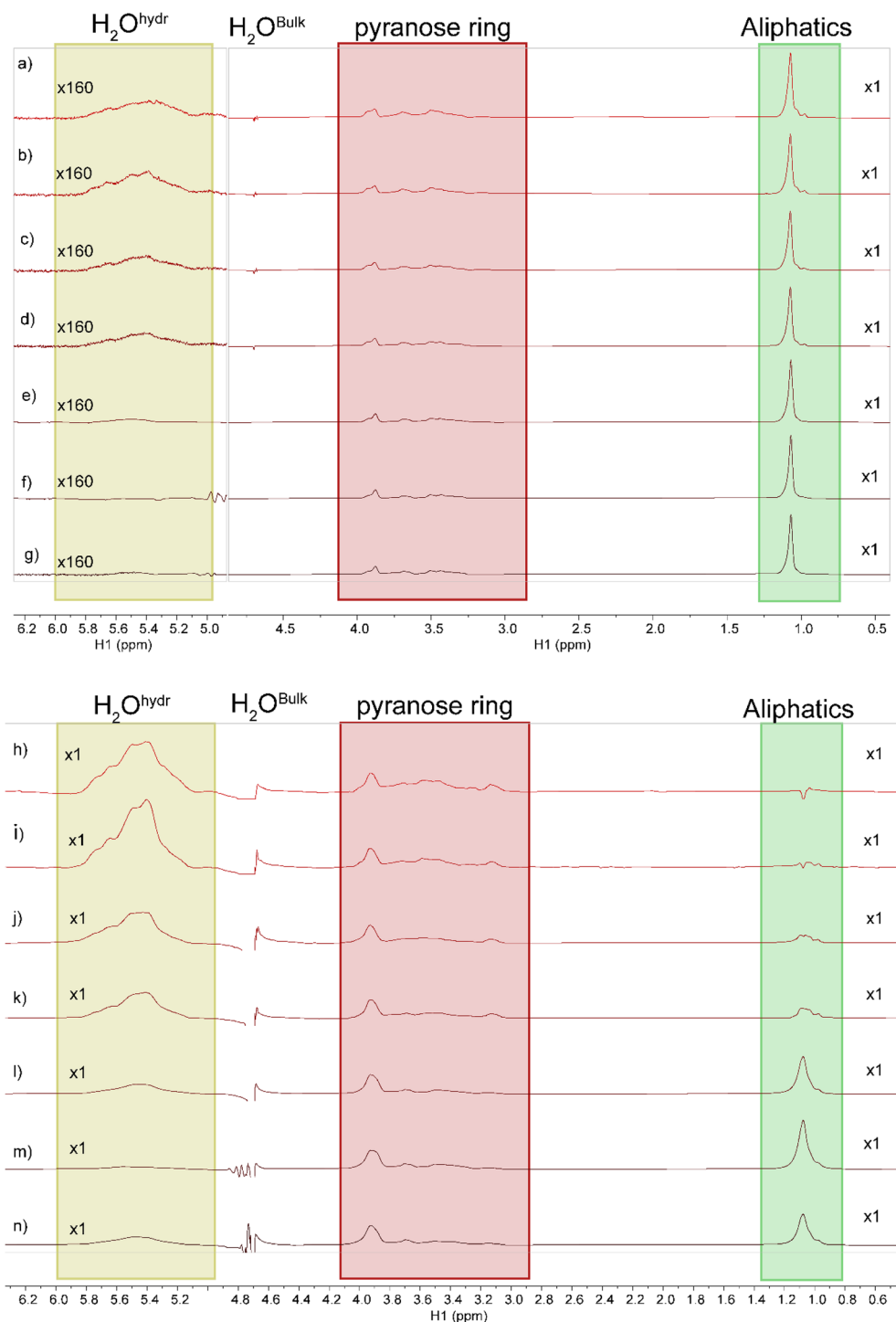
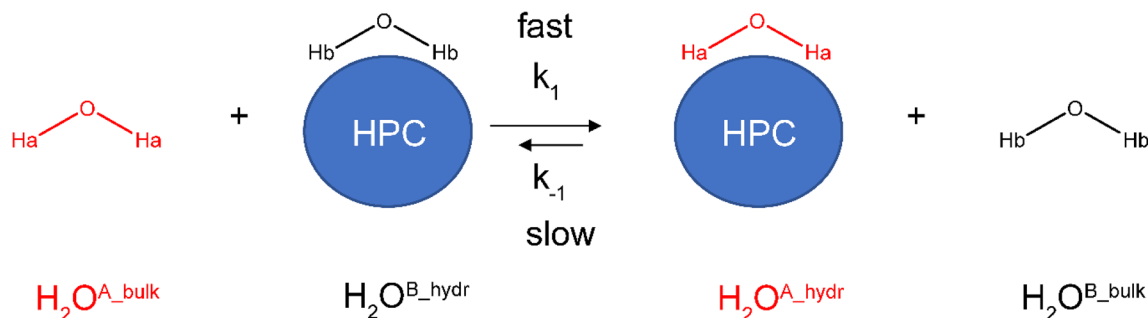


**FIGURE 4** Spectra  $^1\text{H}$  quantitative (top panel) and WaterLOGSY (mixing time of 50 ms) (lower panel) of (a, h) HPC-UL, (b, i) HPC-SSL, (c, j) HPC-SL, (d, k) HPC-L, (e, l) HPC-M, (f, m) HPC-H, and (g, n) HPC-VH dissolved in  $\text{H}_2\text{O}$ . From top to bottom, spectra are arranged in the increasing order of  $M_w$  [Color figure can be viewed at [wileyonlinelibrary.com](http://wileyonlinelibrary.com)]



**SCHEME 1** Water-HPC equilibrium in solution and WaterLOGSY principle. The magnetization of the bulk water molecules  $\text{H}_2\text{O}^{\text{A\_bulk}}$  is selectively taken out of equilibrium (inverted) by WaterLOGSY. Following equilibrium,  $\text{H}_2\text{O}^{\text{A\_bulk}}$  molecules are introduced to the hydration layer of HPC, and previous water molecules  $\text{H}_2\text{O}^{\text{B\_hydr}}$  are ejected. Observable intermolecular NOEs are generated when the residence time of  $\text{H}_2\text{O}^{\text{A\_hydr}}$  in contact with HPC is sufficiently long, which requires the kinetic condition  $k_1 > k_{-1}$  [Color figure can be viewed at [wileyonlinelibrary.com](http://wileyonlinelibrary.com)]

good water-holding performance and NMR can be used to analyze their water-retention properties and dynamics of water exchange. Two NMR techniques were used in this study, viz.  $^1\text{H}$  quantitative to quantify hydration in closely packed layers and WaterLOGSY analysis<sup>[6]</sup> for information on water dynamics; the latter had been used previously to study of hydration in large biopolymers such as proteins.<sup>[14,15]</sup> All the samples for this study were prepared at a concentration of 1.8%; however,  $\text{H}_2\text{O}$  was used as the solvent instead of  $\text{D}_2\text{O}$ .

Spectra a and b in Figure 4 show the  $^1\text{H}$  quantitative and WaterLOGSY spectra, respectively, of the seven samples studied.

Interestingly, all the spectra included a relatively broad peak in the region of 5–6 ppm, which is not visible in the  $^1\text{H}$  spectrum of the analogous samples prepared in  $\text{D}_2\text{O}$  (for comparison, see the proton spectrum in Figures 1 and 2). The broad peak can be attributed to hydration of water ( $\text{H}_2\text{O}^{\text{hydr}}$ ); its presence denotes molecules of water with a high residence time in contact with the HPC polymer. Spectra a and b in Figure 4 contain a peak corresponding to water at the expected position ( $\sim 4.7$  ppm) and this signal corresponds to the most abundant and undifferentiated bulk water ( $\text{H}_2\text{O}^{\text{bulk}}$ ); its intensity was experimentally suppressed or substantially attenuated to yield a dynamic range to detect other peaks.

Integral quantification in the  $^1\text{H}$  quantitative spectra (a–g in Figure 4) was performed with respect to the reference integral of pyranose ring protons. This calculation provides a relevant parameter that is representative of the aliphatic to pyranose ratio. The obtained results are included in Table 1 and they exhibit a slight and consistent decrease in the total aliphatic chain substitution according to an inverse relationship with HPC  $M_w$ . The increase in the aliphatic content can interfere with the hydration properties of the sample because the extra

steric effects are observed to reduce the accessibility of water to the aliphatic chains even more; this is in contrast with the expected behavior for the highly hydrophilic part of pyranose rings.

WaterLOGSY intensities were modulated by the efficient transfer of magnetization from  $\text{H}_2\text{O}^{\text{bulk}}$  to other types of protons in contact with bulk water. At the shortest mixing time (50 ms) for WaterLOGSY spectroscopy (spectra h–n in Figure 4),  $\text{H}_2\text{O}^{\text{bulk}}$  transfers very little magnetization via NOE to the signals of the pyranose ring protons and even less to the aliphatic protons. Peak intensity corresponding to  $\text{H}_2\text{O}^{\text{hydr}}$  was clearly amplified with respect to other peaks in the same spectrum and even the same peak in the corresponding  $^1\text{H}$  quantitative spectra (a–g in Figure 4). The latter observation implies a remarkable transfer of magnetization from excited  $\text{H}_2\text{O}^{\text{bulk}}$  in WaterLOGSY spectra to  $\text{H}_2\text{O}^{\text{hydr}}$  during the short mixing time (50 ms) used to record the spectra. In between the two possible NOE and chemical exchange mechanisms that contribute to signal intensity in WaterLOGSY spectra, the latter results in considerably faster kinetics and contributes to a large extent to the intensity of the  $\text{H}_2\text{O}^{\text{hydr}}$  peak. Scheme 1 illustrates the mechanism of chemical exchange equilibrium that converts the WaterLOGSY excited signal of  $\text{H}_2\text{O}^{\text{bulk}}$  water into that of  $\text{H}_2\text{O}^{\text{hydr}}$ . This mechanism follows two kinetic constants  $k_1$  and  $k^{-1}$  that follow the relationship  $k^1 \gg k^{-1}$ ; furthermore,  $k_1 > 50$  ms.

The evolution of WaterLOGSY signal intensities at a series of mixing times is represented in Figure 5 for the seven chosen HPC samples.

The peak behavior observed in Figure 5 was extremely similar for all the seven samples. The intensity of the  $\text{H}_2\text{O}^{\text{hydr}}$  peak decayed with an increase in mixing time, which is in agreement with the exchange mechanism proposed in Scheme 1. In contrast, the intensities of

the pyranose ring protons and aliphatic chains increase with an increase in mixing time, which is consistent with the NOE mechanism mediated by the proximity of these protons to the two types of water,  $\text{H}_2\text{O}^{\text{bulk}}$  and more importantly,  $\text{H}_2\text{O}^{\text{hydr}}$ .

Having identified the effects that occur with respect to peak intensity in WaterLOGSY spectra, peak integrals (h)–(n) in Figure 4) were quantified at the lowest mixing time of 50 ms. These calculations yielded two independent parameters related to hydration. One parameter is

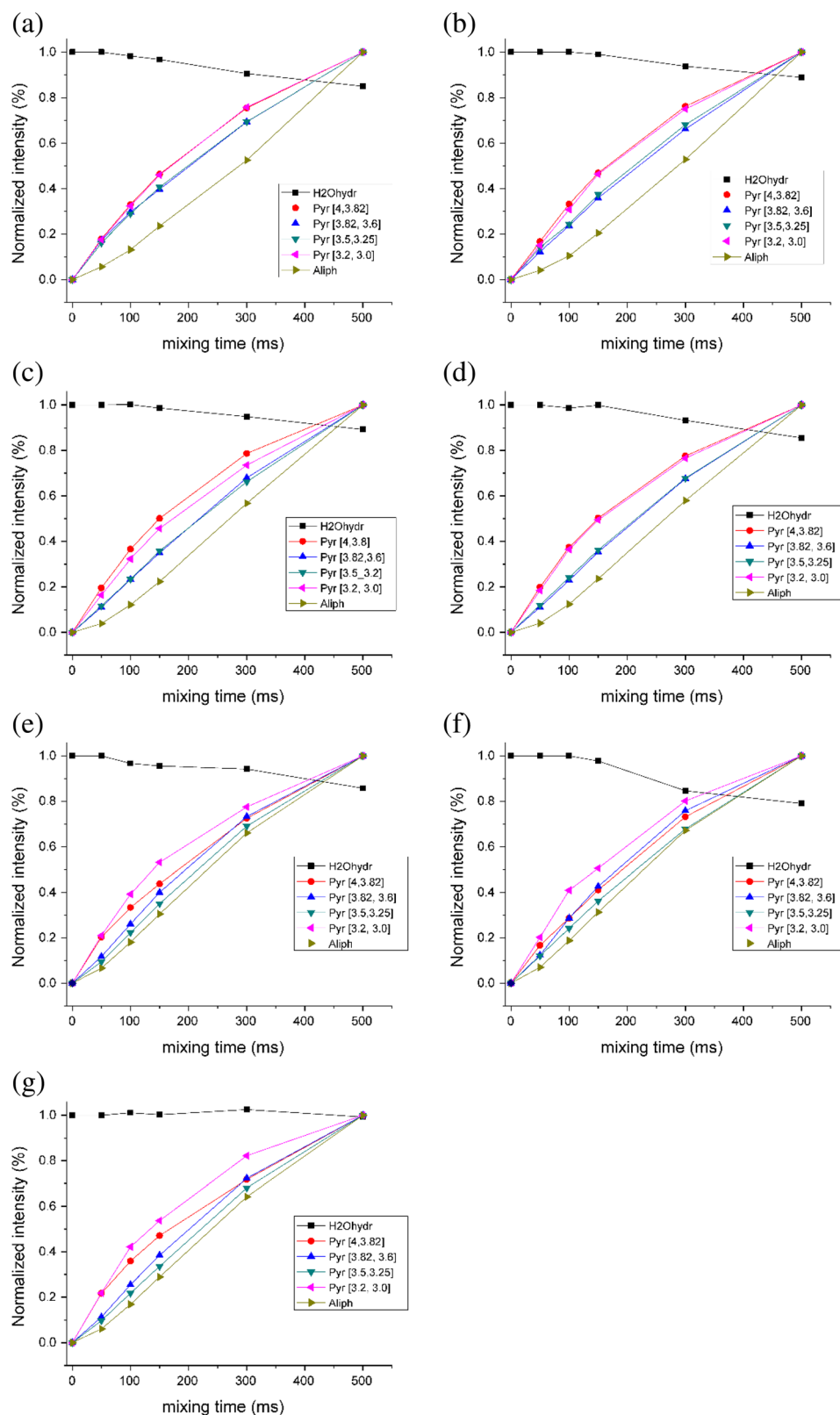


**FIGURE 5** WaterLOGSY intensity build-up plot of signals measured for HPC samples prepared in  $\text{H}_2\text{O}$ . (a) HPC-UL, (b) HPC-SSL, (c) HPC-SL, (d) HPC-L, (e) HPC-M, (f) HPC-H, and (g) HPC-VH. The area corresponding to pyranose ring protons was integrated in four different regions as indicated by parentheses (in ppm) [Color figure can be viewed at [wileyonlinelibrary.com](http://wileyonlinelibrary.com)]



the relative area of peak  $\text{H}_2\text{O}^{\text{hydr}}$  with respect to the total signal area in the same spectrum ( $\%\text{H}_2\text{O}^{\text{hydr}}$ ). The highest values of  $\%\text{H}_2\text{O}^{\text{hydr}}$  (see Table 1) were obtained for HPC samples with a  $M_w$  of 140 kDa or less (81–94%). For those samples with higher  $M_w$ , the values of  $\%\text{H}_2\text{O}^{\text{hydr}}$  were notably lower (1–9%). The second parameter is the relative area of the aliphatic signals with respect to the total signal area in the same spectrum ( $\%\text{aliphatics}$ ). It can be seen in Table 1 that the trend of  $\%\text{aliphatics}$  is the opposite of that of  $\%\text{H}_2\text{O}^{\text{hydr}}$ ; a very small  $\%\text{aliphatics}$  value was observed at  $M_w$  values 140 kDa or lower (0–8%) while notably high values were obtained at higher  $M_w$  values (36–94%).

The trends observed for  $\%\text{H}_2\text{O}^{\text{hydr}}$  and  $\%\text{aliphatics}$  can be explained as follows;  $\text{H}_2\text{O}^{\text{hydr}}$  reflects the amount of water that the polymer is able to introduce in the solvation layer of the HPC structure. It must be disposed toward the external side of the polymer to ensure that  $\text{H}_2\text{O}^{\text{hydr}}$  can exchange with external bulk water. As the length of the HPC polymer chain increases, the contribution of  $\%\text{H}_2\text{O}^{\text{hydr}}$  becomes less relevant because other parts of the HPC structure contribute more to water retention; in particular, the effect of aliphatic residues, expressed by  $\%\text{aliphatics}$  in Table 1, becomes the most prominent factor at  $M_w > 140$  kDa. This observation can be explained by considering that the hydrophobicity of aliphatic residues of HPC can lead to the formation of stable vesicles on the interior side of the HPC polymer. These vesicles can retain a substantial amount of water without exchanging with the bulk water located on the exterior side.

The curves in Figure 5 for the seven chosen HPC samples corresponding to the pyranose protons are observed to be above the curves of the aliphatic protons, which indicate that the former are more exposed to the water.

## 4 | CONCLUSIONS

In this work, we applied liquid NMR methods to study HPC samples in equilibrium-swollen gels prepared at a constant concentration in the low-viscosity regime.<sup>[11]</sup> The results obtained herein are consistent and complement the previous studies on HPC, which shows that solubility is enhanced for short-chain grades.<sup>[1–3]</sup> In this work, we find that the water retention of HPC, and therefore its drug solubility, is modulated primarily by the polymer chain length ( $M_w$ ) and the aliphatic chain content. Evidently, HPCs with the lowest molecular weights (UL and SSL) exhibit an association with the fact that they comprise the lowest amount of water molecules around their polymer chains; this is probably because they do not allow significant vesicle formation and consequently, exhibit substantially low agglomeration. This

phenomenon could “facilitate” the interaction between HPC-UL and SSL, thus preventing the precipitation of small hydrophobic molecules in aqueous solutions.

Previous methods for studying HPC hydration based on NMR longitudinal ( $T_1$ ) and transverse ( $T_2$ ) parameters have analyzed the bulk water peak, and different types of water ordering in hydrogels of HPC were reported. These studies found two types of water molecules, bulk-like water (freezable water at 0°C) and water weakly interacting with macromolecules (nonfreezable water at 0°C).<sup>[16]</sup> The method proposed in this work, which relies on VT  $^1\text{H}$ -quantitative and WaterLOGSY spectra, is consistent with those findings and has permitted the detection of two independent resonances for the bulk water and hydrated water (Figure 4). These findings reflect the differences in the magnetic susceptibility between the environments of the two hydration modes, which are in slow exchange on the chemical shift timescale under our experimental conditions.

Studies based on MRI and NMR relaxation have detected a gradient of water mobility across the gel layer and different degrees of polymer hydration at different depths in the gel.<sup>[17]</sup> However, the WaterLOGSY used in this work is sensitive only to direct molecular contact between water and HPC. This sensitivity implies that the peak intensity in the WaterLOGSY spectrum specifically reflects the fraction of bulk water with sufficient accessibility to penetrate into the first hydration shell of HPC (Scheme 1), which has obvious implications for the characterization of HPCs as drug-delivery systems.

Solution NMR is known to have limitations with respect to the maximum size of the HPC molecule or aggregate that can be studied; in this sense, our results are skewed toward those parts along the HPC chain that exhibit a sufficient molecular mobility, which are exactly the parts that are more exposed to the surrounding water. Future works for employing solid NMR can provide the complementary information regarding the most rigid parts of HPC as a function of water content.

## ORCID

Edmont Stoyanov  <https://orcid.org/0000-0002-1571-9259>

## REFERENCES

- [1] A. Ito, C. Konnerth, J. Schmidt, W. Peukert, *Eur. J. Pharm. Biopharm.* **2016**, 98, 98.
- [2] C. Konnerth, F. Flach, S. Breitung-Faes, C. Damm, J. Schmidt, A. Kwade, W. Peukert, *Powder Technol.* **2016**, 294, 71.
- [3] D. E. Zecevic, R. Meier, R. Daniels, K. G. Wagner, *Eur. J. Pharm. Biopharm.* **2014**, 87, 264.
- [4] K. Kimura, T. Shigemura, M. Kubo, Y. Maru, *Makromol. Chem. Macromol. Chem. Phys.* **1985**, 186, 61.
- [5] D. Desai, F. Rinaldi, S. Kothari, S. Paruchuri, D. Li, M. Lai, S. Fung, D. Both, *Int. J. Pharm.* **2006**, 308, 40.

- [6] C. Dalvit, G. Fogliatto, A. Stewart, M. Veronesi, B. Stockman, *J. Biomol. NMR* **2001**, *21*, 349.
- [7] D. H. Wu, A. D. Chen, C. S. Johnson, *J. Magn. Reson. Ser. A* **1995**, *115*, 260.
- [8] R. W. Adams, C. M. Holroyd, J. A. Aguilar, M. Nilsson, G. A. Morris, *Chem. Commun.* **2013**, *49*, 358.
- [9] N. Sarkar, *J. Appl. Polym. Sci.* **1979**, *24*, 1073.
- [10] S. Constanzo, R. Pasquino, R. Donato, N. Grizzuti, *Polymer* **2017**, *132*, 157.
- [11] K. S. Hossain, K. Miyana, H. Maeda, N. Nemoto, *Biomacromolecules* **2001**, *2*, 442.
- [12] S. Viel, D. Capitani, L. Mannina, A. Segre, *Biomacromolecules* **2003**, *4*, 1843.
- [13] R. Novoa-Carballal, R. Riguera, E. Fernandez-Megia, *Mol. Pharm.* **2013**, *10*, 3225.
- [14] C. Ludwig, P. J. Michiels, X. Wu, K. L. Kavanagh, E. Pilka, A. Jansson, U. Oppermann, U. L. Günther, *J. Med. Chem.* **2008**, *51*, 1.
- [15] L. Geist, M. Mayer, X. L. Cockcroft, B. Wolkerstorfer, D. Kessler, H. Engelhardt, D. B. McConnell, R. Konrat, *J. Med. Chem.* **2017**, *21*, 8708.
- [16] I. Katzhendler, K. Mäder, M. Friedman, *Int. J. Pharm.* **2000**, *200*, 161.
- [17] A. R. Rajabi-Siahboomi, R. W. Bowtell, P. Mansfield, M. C. Davies, C. D. Melia, *Pharm. Res.* **1997**, *13*, 376.

**How to cite this article:** Martin-Pastor M, Stoyanov E. Mechanism of interaction between hydroxypropyl cellulose and water in aqueous solutions: Importance of polymer chain length. *J Polym Sci.* 2020;58:1632–1641. <https://doi.org/10.1002/pol.20200185>